numerical simulations. The excellent quality of the interferometric fringe patterns obtained from the AF-ESPI method is demonstrated. In Figs. 3–5, we indicate the phase of displacement in finite element results with a + or − sign. The regions of the same sign have in-phase motion, and nodal lines (thick black lines) are also shown in Figs. 3–5. The brightest fringes on the experimental results represent the nodal lines of the vibrating cracked plate at resonant frequencies. The rest of the fringes are contours of constant displacement. It can be seen that the vibration mode shapes obtained experimentally agree very well with those obtained from the finite element method.

The related amplitude $A_i, i = 1, 2, 3, \ldots, n$, for the ith fringe in the experimental results can be quantitatively calculated by the roots R_i of $J_0(\Gamma A_i) = 0$. The first 10 roots R_i for $J_0(R_i) = 0$ are 2.4, 5.52, 8.65, 11.79, 14.93, 18.07, 21.21, 24.35, 27.49, and 30.63. The correspondent amplitude A_i of the out-of-plane displacement can be evaluated by the following equation:

$$A_i = \frac{\lambda R_i}{2\pi(1 + \cos\theta)} \tag{3}$$

We use $\theta = 10$ deg for the experimental setup and $\lambda = 632.8$ nm; the related amplitudes for the first 10 dark fringes are $A_i, i = 1 \sim 10, = 0.12$, 0.28, 0.44, 0.6, 0.76, 0.92, 1.08, 1.24, 1.41, and 1.57 μm. The maximum value of the vibration displacement and related amplitudes of some fringes in the experimental results are indicated in Figs. 3–5. Note that the vibration displacements obtained in this study are in the order of a micrometer.

Because the crack will introduce a new free boundary of the cantilever plate, the mode shape of a cracked plate is complicated and quite different from that of a plate without a crack. A complete discussion of out-of-plane vibration mode shapes for different boundary conditions of isotropic plates without cracks was presented by Huang and Ma.[7] The vibrating mode shapes of the first and the second modes shown in Figs. 3–5 are pure bending and torsion modes, respectively. The mode shapes for long cracks (Figs. 4 and 5; $a = 35$ and 50 mm) are similar, but they are quite different if compared with mode shapes for the short crack (Fig. 3; $a = 20$ mm). Note that the displacements along the crack surface for the first 10 modes are all in-phase for the short crack and that the nodal lines will not pass the crack surface. However, the nodal lines of modes 7 and 9 for long cracks are terminated at the crack surface.

III. Conclusions

Investigation of the vibration problem by employing the ESPI method has the advantages of real-time and noncontact measurement, submicron sensitivity, digital image processing, and so on. In this Note, a self-arranged AF-ESPI optical setup with good fringe visibility and noise reduction was established to obtain the resonant frequencies and corresponding mode shapes of cantilever cracked plates at the same time. Compared with the spectrum analysis method or modal analysis method, AF-ESPI is more convenient in experimental measurement, and excellent quality of the interferometric fringe patterns are obtained. Numerical calculations of resonant frequencies and mode shapes based on a finite element package are also performed, and good agreement is obtained in comparison with experimental measurements. The influence of the crack length on the vibration behavior of the cantilever cracked plate is discussed in detail. Note that frequencies obtained experimentally are typically lower than theoretical ones because one cannot get the perfectly rigid clamping condition.

Acknowledgment

The authors thank the National Science Council (NSC) of the Republic of China for supporting this research under Grant NSC 87-2218-E002-022.

References

[1]Rastogi, P. K., *Holographic Interferometry*, Springer-Verlag, Berlin, 1994.

[2]Butters, J. N., and Leendertz, J. A., "Speckle Pattern and Holographic Techniques in Engineering Metrology," *Optics Laser Technology*, Vol. 3, No. 1, 1971, pp. 26–30.

[3]Wang, W. C., Hwang, C. H., and Lin, S. Y., "Vibration Measurement by the Time-Averaged Electronic Speckle Pattern Interferometry Methods," *Applied Optics*, Vol. 35, No. 22, 1996, pp. 4502–4509.

[4]Ma, C. C., and Huang, C. H., "The Investigation of Three-Dimensional Vibration for Piezoelectric Rectangular Parallelepipeds Using the AF-ESPI Method," *IEEE Transactions on Ultrasonics, Ferroelectrics, and Frequency Control*, Vol. 48, No. 1, 2001, pp. 142–153.

[5]Huang, C. H., and Ma, C. C., "Vibration Characteristics for Piezoelectric Cylinders Using Amplitude-Fluctuation Electronic Speckle Pattern Interferometry," *AIAA Journal*, Vol. 36, No. 12, 1998, pp. 2262–2268.

[6]"ABAQUS User's Manual," Ver. 5.5, Hibbit, Karlsson, and Sorensen, Inc., Pawtucket, RI, 1995.

[7]Huang, C. H., and Ma, C. C., "Experimental Measurement of Mode Shapes and Frequencies for Vibration of Plates by Optical Interferometry Method," *Journal of Vibration and Acoustics*, Vol. 123, No. 2, 2001, pp. 276–280.

A. M. Waas
Associate Editor

Static and Dynamic Validations of a Refined Thin-Walled Composite Beam Model

Zhanming Qin* and Liviu Librescu†
Virginia Polytechnic Institute and State University, Blacksburg, Virginia 24061-0219

I. Introduction

THE increasing need for weight saving and structural efficiency of aerospace vehicles has prompted wide use of thin-walled beam structures.[1] At the same time, due to the increased importance of composite materials in the design of aerospace vehicles, the concept of anisotropic thin-walled beam model has reached special prominence in the last two decades.[1,2] However, in contrast to the metallic structures, the composite structures exhibit significant nonclassical effects such as transverse shear, warping restraint, three-dimensional strain effect, and contourwise shear stiffness variations. Toward a reliable design, these effects should be accounted for and assessed even in the predesign process. In fact, in the past years, a number of analytical models of anisotropic thin-walled beams have been proposed and validated either numerically or in light of the experimental evidence.[2] On the other hand, although a refined thin-walled beam theory originally developed by Song[3] and Librescu and Song[1] has been extensively used for the study, among others, of dynamic response/structural feedback control[3–10] and static aeroelasticity,[3,7,11,12] no validations of it against the experimental, analytical, or numerical predictions obtained within other thin-walled beam models are available in literature. Within the frame of this refined model, some effects such as the three-dimensional strain effect[13,14] and nonuniformity effect of contourwise shear stiffness, that are also usually significant for the laminated composite beams[2,13–15] and were not formerly accounted for, are further incorporated, and the model hereby developed is investigated against the available data from experiments, finite element method, and other analytical models.

II. Theory

A single-cell, closed cross section, fiber-reinforced composite thin-walled beam is considered. The coordinate system that is

Received 3 January 2001; revision received 20 August 2001; accepted for publication 21 August 2001.

*Graduate Teaching Assistant, Department of Engineering Science and Mechanics. Student Member AIAA.

†Professor, Department of Engineering Science and Mechanics.

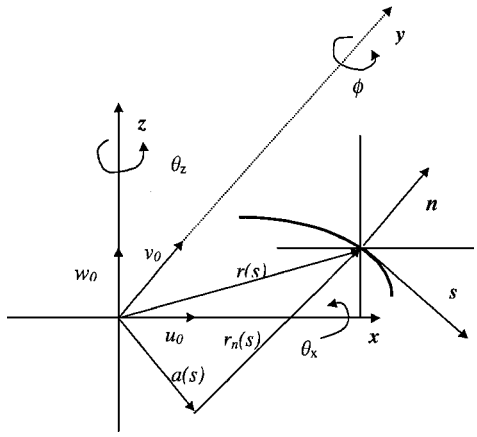

Fig. 1 Coordinate system and displacement field for the beam model.

usually used in the analyses of aircraft wings is adopted (Fig. 1). Based on the basic assumptions formulated in Refs. 1 and 3, the following representation of the three-dimensional displacement quantities is postulated:

$$u(x, y, z, t) = u_0(y, t) + z\phi(y, t)$$

$$w(x, y, z, t) = w_0(y, t) - x\phi(y, t) \tag{1a}$$

$$v(x, y, z, t) = v_0(y, t) + \left[x(s) - n\frac{\mathrm{d}z}{\mathrm{d}s}\right]\theta_z(y, t)$$

$$+ \left[z(s) + n\frac{\mathrm{d}x}{\mathrm{d}s}\right]\theta_x(y, t) - [F_w(s) + na(s)]\phi'(y, t) \tag{1b}$$

where

$$\theta_x(y, t) = \gamma_{yz}(y, t) - w_0'(y, t)$$

$$\theta_z(y, t) = \gamma_{xy}(y, t) - u_0'(y, t), \qquad a(s) = -\left(z\frac{\mathrm{d}z}{\mathrm{d}s} + x\frac{\mathrm{d}x}{\mathrm{d}s}\right) \tag{2}$$

In the preceding expressions, $\theta_x(y, t)$, $\theta_z(y, t)$, and $\phi(y, t)$ are the rotations of the cross section about the axes x and z and the twist about the y axis, respectively; $\gamma_{yz}(y, t)$ and $\gamma_{xy}(y, t)$ are the transverse shear strain measures, and $F_w(s)$ is the warping function expressed as

$$F_w(s) = \int_0^s [r_n(s) - \psi(s)]\,\mathrm{d}s \tag{3}$$

in Eq. (3), the torsional function $\psi(s)$ and the quantity $r_n(s)$ are expressed as

$$\psi(s) = \oint_C r_n(\bar{s})\,\mathrm{d}\bar{s} \Big/ h(s)G_{sy}(s)\oint_C \frac{\mathrm{d}\bar{s}}{h(\bar{s})G_{sy}(\bar{s})}$$

$$r_n(s) = z\frac{\mathrm{d}x}{\mathrm{d}s} - x\frac{\mathrm{d}z}{\mathrm{d}s} \tag{4}$$

where $G_{sy}(s)$ is the effective membrane shear stiffness, which is defined as[13]

$$G_{sy}(s) = \frac{N_{sy}}{h(s)\gamma_{sy}^0(s)} \tag{5}$$

Notice that for the thin-walled beam theory considered herein, the six kinematic variables, $u_0(y, t)$, $v_0(y, t)$, $w_0(y, t)$, $\theta_x(y, t)$, $\theta_z(y, t)$, and $\phi(y, t)$, that represent one-dimensional displacement measures constitute the basic unknown quantities of the problem. When transverse shear effects are ignored, Eq. (2) degenerates to $\theta_x = -w_0'$ and $\theta_z = -u_0'$, and as a result, the number of the basic unknown quantities reduces to four. Such a case leads to the classical, unshearable beam model.

Based on the assumption related to the three-dimensional strain effect, the stress resultants and stress couples can be reduced to the following expressions:

$$\begin{Bmatrix} N_{yy} \\ N_{sy} \\ L_{yy} \\ L_{sy} \end{Bmatrix} = \begin{bmatrix} K_{11} & K_{12} & K_{13} & K_{14} \\ K_{21} & K_{22} & K_{23} & K_{24} \\ K_{41} & K_{42} & K_{43} & K_{44} \\ K_{51} & K_{52} & K_{53} & K_{54} \end{bmatrix} \begin{Bmatrix} \varepsilon_{yy}^0 \\ \gamma_{sy}^0 \\ \phi' \\ \varepsilon_{yy}^n \end{Bmatrix} \tag{6a}$$

$$N_{ny} = \left[A_{44} - A_{45}^2/A_{55}\right]\gamma_{ny} \tag{6b}$$

in which K_{ij} are the reduced stiffness coefficients, ε_{yy}^0 and ε_{yy}^0 are the axial strain components associated with the primary and secondary warping, respectively; and γ_{sy}^0 is a measure corresponding to the transformed transverse shear strain in the local coordinate system (s, y, n).

The one-dimensional stress resultant and stress couple measures are defined as follows:

$$T_y(y, t) = \oint_C N_{yy}\,\mathrm{d}s, \qquad M_z(y, t) = \oint_C \left(xN_{yy} - L_{yy}\frac{\mathrm{d}z}{\mathrm{d}s}\right)\mathrm{d}s$$

$$M_x(y, t) = \oint_C \left(zN_{yy} + L_{yy}\frac{\mathrm{d}x}{\mathrm{d}s}\right)\mathrm{d}s$$

$$Q_x(y, t) = \oint_C \left(N_{sy}\frac{\mathrm{d}x}{\mathrm{d}s} - N_{ny}\frac{\mathrm{d}z}{\mathrm{d}s}\right)\mathrm{d}s$$

$$Q_z(y, t) = \oint_C \left(N_{sy}\frac{\mathrm{d}z}{\mathrm{d}s} + N_{ny}\frac{\mathrm{d}x}{\mathrm{d}s}\right)\mathrm{d}s$$

$$B_w(y, t) = -\oint_C [F_w(s)N_{yy} + a(s)L_{yy}]\,\mathrm{d}s$$

$$M_y(y, t) = \oint_C N_{sy}\psi(s)\,\mathrm{d}s \tag{7}$$

For general anisotropic and heterogeneous materials, the stiffness matrix that correlates the one-dimensional stress resultants and stress couples T_y, $M_z, \ldots, M_y$, where the one-dimensional strain measures are fully populated. This results in completely coupled governing systems implying that the motions hereby described, namely, the lateral and vertical transverse bendings, the twist, the extension, the transverse shearing and the warping, are fully coupled. However, for the purpose of validation, the following special cases yielding special elastic couplings will be investigated, namely, 1) the cross-ply layup, 2) the circumferentially uniform stiffness (CUS) layup (also refered to as the anti-symmetric layup[15]), and 3) the circumferentially asymmetric stiffness (CAS) layup (also referred to as the symmetric layup[15]). All of the validations are on the thin-walled box beams.

The governing equations and the associated boundary conditions for these special layups in terms of the basic unknowns are then obtained via Hamilton's principle. The extended Galerkin's method (EGM) (see Refs. 9 and 16) is used for the actual numerical solution. As for the material properties of thin-walled beams used in the validation of static response, these are summarized in Table 2 of Ref. 17, the geometric specification of the beams is summarized in Table 2 of Ref. 14, and the layups are specified in Table 3 of Ref. 14. The material, geometric, and layup specifications used in the validation of dynamic characteristics of the thin-walled beams are listed in Table 1 of Ref. 18. Note that, for the purpose of convenience, the ply angle in this Note is defined in Ref. 14.

III. Validation and Discussion

Both the static response and eigenfrequency characteristics are investigated. Figure 2 shows the influence of nonuniformity of shear stiffness G_{sy} on the bending slope of the CAS3 test beam (defined in Ref. 14) subject to a tip torque. In this case, the uniform shear model predicts only 50% of the deformation as predicted by the nonuniform counterpart. A similar phenomenon (the significant

Table 1 Dynamic validation: comparison of the natural frequencies

Layup	Mode no.	Experiment,[a] Ref. 18	Analytical, Ref. 17	Difference with experiment data, %	Present	Difference with experiment data, %
$[30]_6$ CAS	1	20.96	19.92	−4.96	21.8	4.00
	2	128.36	124.73	−2.83	123.28	−3.96
$[45]_6$ CAS	1	16.67	14.69	−11.88	15.04	−9.78
	2	96.15	92.02	−4.30	92.39	−3.91

[a]Data are obtained from Ref. 18 that are also listed in Ref. 17.

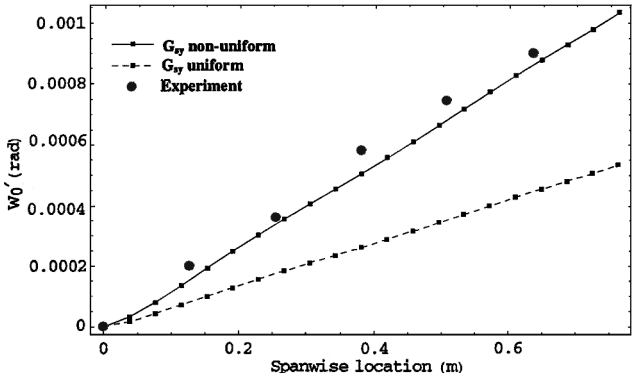

Fig. 2 Influence of shear variation on the bending slope of the CAS3 test beam by 0.113 N · m tip torque (for the source of the experimental data, see Ref. 14).

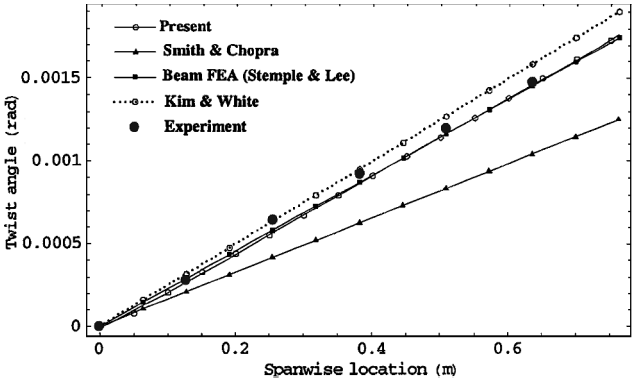

Fig. 3 Twist angle of the CAS3 beam by 0.113 N · m tip torque (for the source of the experimental data and finite element analysis result, see Ref. 14).

discrepancy) was also reported by Smith and Chopra.[15] Figure 2 also clearly demonstrates that incorporation of the nonuniformity of the shear stiffness within the earlier developed refined thin-walled beam model has a potential to significantly improve its prediction accuracy.

Figure 3 supplies the twist angle prediction of a thin-walled beam featuring the CAS3 configuration. The displayed comparison reveals that the present prediction is in excellent agreement with the ones provided by experiments and the finite element method.

Compared with the static validation, for the purpose of dynamic validation of thin-walled beam models, there are very few experimental data available in the literature. Table 1 lists some results of natural frequencies predicted by the present model. Results show that the present model yields good agreement with the experimental data. Notice that consistent lower predictions of the natural frequencies of the CAS test beams listed in this Note are obtained by the analytical model by Armanios and Badir,[17] even though the transverse shear effect was not included in the latter model.

IV. Conclusions

Within the framework of an existing refined thin-walled beam model, the three-dimensional strain effect and the nonuniformity of the contourwise shear effect are further incorporated, and the model hereby developed is investigated. Validation results obtained by the present model reveal the excellence of predictions when comparing these results with some of the experimental data available in the literature. Because of the limited space available, many other results highlighting the high accuracy of the predictions provided by this model and also the emerging conclusions have not been presented. These results will be presented elsewhere.

References

[1]Librescu, L., and Song, O., "Behavior of Thin-Walled Beams Made of Advanced Composite Materials and Incorporating Non-Classical Effects," *Applied Mechanics Reviews*, Vol. 44, No. 11, 1991, pp. S174–S180.

[2]Jung, S. N., Nagaraj, V. T., and Chopra, I., "Assessment of Composite Rotor Blade Modeling Techniques," *Journal of the American Helicopter Society*, Vol. 44, No. 3, 1999, pp. 188–205.

[3]Song, O., "Modeling and Response Analysis of Thin-Walled Beam Structures Constructed of Advanced Composite Materials," Ph.D. Dissertation, Virginia Polytechnic Inst. and State Univ., Blacksburg, VA, 1990.

[4]Na, S. S., and Librescu, L., "Oscillation Control of Cantilevers via Smart Materials Technology and Optimal Feedback Control: Actuator Location and Power Consumption Issues," *Smart Material and Structures*, Vol. 7, 1998, pp. 833–842.

[5]Librescu, L., and Na, S. S., "Dynamic Response Control of Thin-Walled Beams to Blast Pulses Using Structural Tailoring and Piezoelectric Actuation," *Journal of Applied Mechanics*, Vol. 65, No. 2, 1998, pp. 497–504.

[6]Song, O., and Librescu, L., "Free Vibration of Anisotropic Composite Thin-Walled Beams of Closed Cross-Section Contour," *Journal of Sound and Vibration*, Vol. 167, No. 1, 1993, pp. 129–147.

[7]Librescu, L., Meirovitch, L., and Song, O., "Refined Structural Modeling for Enhancing Vibrations and Aeroelastic Characteristics of Composite Aircraft Wings," *La Recherche Aérospatiale*, No. 1, 1996, pp. 23–35.

[8]Librescu, L., Meirovitch, L., and Song, O., "Integrated Structural Tailoring and Control Using Adaptive Materials for Advanced Aircraft Wings," *Journal of Aircraft*, Vol. 33, No. 1, 1996, p. 1996.

[9]Librescu, L., Meirovitch, L., and Na, S. S., "Control of Cantilevers Vibration via Structural Tailoring and Adaptive Materials," *AIAA Journal*, Vol. 35, No. 8, 1997, pp. 1309–1315.

[10]Librescu, L., Song, O., and Rogers, C. A., "Adaptive Vibrational Behavior of Cantilevered Structures Modeled as Composite Thin-Walled Beams," *International Journal of Engineering Science*, Vol. 31, No. 5, 1993, pp. 775–792.

[11]Librescu, L., and Song, O., "On the Static Aeroelastic Tailoring of Composite Aircraft Swept Wings Modeled as Thin-Walled Beam Structures," *Composites Engineering*, Vol. 2, 1992, pp. 497–512.

[12]Song, O., Librescu, L., and Rogers, C. A., "Application of Adaptive Technology to Static Aeroelastic Control of Wing Structures," *AIAA Journal*, Vol. 30, No. 12, 1992, pp. 2882–2889.

[13]Bhaskar, K., and Librescu, L., "A Geometrically Non-Linear Theory for Laminated Anisotropic Thin-Walled Beams," *International Journal of Engineering Science*, Vol. 33, No. 9, 1995, pp. 1331–1344.

[14]Kim, C., and White, S. R., "Thick-Walled Composite Beam Theory Including 3-D Elastic Effects and Torsional Warping," *International Journal of Solids and Structures*, Vol. 34, No. 31–32, 1997, pp. 4237–4259.

[15]Smith, E. C., and Chopra, I., "Formulation and Evaluation of an Analytical Model for Composite Box-Beams," *Journal of the American Helicopter Society*, Vol. 36, No. 3, 1991, pp. 23–35.

[16]Palazotto, A. N., and Linnemann, P. E., "Vibration and Buckling Characteristics of Composite Cylindrical Panels Incorporating the Effects of a Higher Order Shear Theory," *International Journal of Solids and Structures*, Vol. 28, No. 3, 1991, pp. 341–361.

[17]Armanios, E. A., and Badir, A. M., "Free Vibration Analysis of Anisotropic Thin-Walled Closed-Section Beams," *AIAA Journal*, Vol. 33, No. 10, 1995, pp. 1905–1910.

[18]Chandra, R., and Chopra, I., "Experimental–Theoretical Investigation of the Vibration Characteristics of Rotating Composite Box Beams," *Journal of Aircraft*, Vol. 29, No. 4, 1992, pp. 657–664.

A. N. Palazotto
Associate Editor